ISSN 0001-4338, Izvestiya, Atmospheric and Oceanic Physics, 2010, Vol. 46, No. 3, pp. 369–378. © Pleiades Publishing, Ltd., 2010.
Original Russian Text © M.V. Kosnik, V.A. Dulov, V.N. Kudryavtsev, 2010, published in Izvestiya AN. Fizika Atmosfery i Okeana, 2010, Vol. 46, No. 3, pp. 400–410.

Generation Mechanisms for Capillary–Gravity Wind Wave Spectrum

M. V. Kosnik, V. A. Dulov, and V. N. Kudryavtsev

Marine Hydrophysical Institute, National Academy of Sciences of Ukraine, ul. Kapitanskaya 4/111, Sevastopol, Crimea, 99011 Ukraine

e-mail: mvkosnik@gmail.com

Received April 28, 2009; in final form, July 27, 2009

Abstract—We investigate the role of different physical mechanisms in the generation of the capillary–gravity wind wave spectrum. This spectrum is calculated by integrating a nonstationary kinetic equation until the solution becomes stready. The mechanisms of spectrum generation under consideration include three-wave interactions, viscous dissipation, energy influx from wind, nonlinear dissipation, and the generation of a parasitic capillary ripple. The three-wave interactions are taken into account as an integral of collisions without additional simplifications. It is shown that the three-wave interactions lead to solution instability if the kinetic equation takes into account only linear sources. To stabilize the solution, the kinetic equation should incorporate a nonlinear dissipation term, which in the range of short gravity waves corresponds to energy losses during wave breaking and microscale wave breaking. In the range of capillary waves, the account of nonlinear dissipation is also needed to ensure a realistic level of the spectrum for large wind velocities. For the steady-state spectrum, the role of three-wave interactions remains essential merely in the range of the minimum of phase velocity, where a trough on the curvature spectrum is formed. At the remaining intervals of the spectrum, the main contribution into the spectral energy balance is provided by the mechanisms of wave injection, nonlinear dissipation, and the generation of parasitic capillaries.

DOI: 10.1134/S0001433810030102

1. INTRODUCTION

Short wind waves of lengths from a millimeter to tens of centimeters determine the heat and momentum fluxes at the sea surface and they generate ocean-surface images in almost the whole range of electromagnetic waves (including the radiowave range) used for space observations of the ocean [1, 2]. The spatial distribution of the spectral density of short waves reflects the wind-velocity field, the presence or absence of films on the sea surface, and mesoscale subsurface processes (fronts, internal waves, and convergence zones) [2]. The account of short waves seems to be essential for estimating the rate of gas exchange through the water surface [3] and for calculating the surface drift velocity, because short waves contribute to the turbulence in the water layer adjacent to the surface [4]. For quantitative investigations of the problems mentioned above, it is necessary to know the spectral density of short wind waves.

The given wave range corresponds to the gravity–capillary (GC) interval, where the effects and forces of gravity and surface tension are important. This leads to the fact that the dynamics of the GC interval differs from that of gravity waves with lengths of a decimeter and more. The GC interval involves three-wave interactions, while only wave quads can resonantly interact in the gravity interval. Accordingly, the nonlinear transport of energy in the gravity interval as compared to the GC interval has the following order of smallness with respect to wave steepness. If the importance of nonlinear transport in the gravity interval is commonly accepted [5], one can expect that, in the GC interval, three-wave interactions will be one of the main factors generating the wave spectrum.

Theoretical investigations of three-wave interactions were performed in a series of works ([6–12], etc.; a more detailed list can be found in [12]). In [6] it was shown that the waves in the capillary interval can exist in an inertial Kolmogorov regime when the spectrum form is determined only three-wave interactions of capillary waves. In [9, 10] it was revealed that, in the case of real seas, the three-wave interactions of gravity and capillary waves (nonlocal interactions) turn out to be more important for spectrum generation in the capillary interval than the three-wave interactions of only capillary waves. The exact numerical calculation of the integral of collisions is a cumbersome problem requiring large machine-time costs. Algorithms of its calculation were proposed independently in [9, 11], where the link between the integral of collisions and the form of the spectrum was also considered. A systematic numerical study of the effects of three-wave interactions in the GC interval was performed in [12]. In [7,

8, 12], the factors of spectrum generation were taken to be the energy influx from wind and its dissipation due to molecular viscosity (in addition to three-wave interactions). However, in the GC interval, the nonlinear dissipation of energy due to microscale wave breaking and the resulting generation of a parasitic capillary ripple appear to be also important [13, 14]. These processes give a direct transfer of energy from gravity to capillary waves, like the nonlocal three-wave interactions; however, their relative role in the spectrum generation remains unclear. Therefore, considering three-wave interactions with the simultaneous account of all the mechanism listed above turns out to be a necessary step in the physical understanding of the dynamics of the GC interval of wind waves.

However, this problem is nontrivial not only due to the complexity of the numerical calculation of three-wave interactions. As was revealed in [12], the three-wave processes along with wind input lead to the instability of the spectrum of GC interval waves. If the model uses mathematical expressions for describing the wave injection, nonlinear dissipation, and the generation of parasitic ripple (which were found independently on the basis of semi-empiric and phenomenological approaches), the model stability in the general case cannot be guaranteed. Thus, successful numerical modeling requires that all spectral influxes–sinks of energy added to three-wave interactions must be such that their combined effect yields spectrum stability.

The mechanisms of energy influxes and sinks added to three-wave interactions were discussed in detail in [14, 15], where the authors also proposed their formalized models based on a generalization of experimental data on the spectra of wind waves in the GC interval. Applying these models yields a semi-empiric model of the spectrum of short wind waves for different wind velocities [14, 15]. The model efficiency can be essentially confirmed by considering a series of facts of its consistency with space radar observations of the ocean [16–18].

In this study, we combine the approach of [15] (a realistic description of the main mechanisms of spectrum generation) and [12] (an accurate calculation of the three-wave energy transfer) into a single model of the spectrum of GC waves. The main objective of this paper is to elucidate the role of relevant physical mechanisms in the generation of the spectrum of short wind waves.

2. MAIN RELATIONS

We will make spectrum calculations on the basis of the kinetic equation [2, 5]

$$\frac{dN(k,\theta)}{dt} = \sum_i Q_i(k,\theta), \qquad (1)$$

where $N(k, \theta) = E(k, \theta)/\omega(k) = \rho c(k) F(k, \theta)$ is the spectral density of the wave action related to the spectra $E(k, \theta)$ of the wave energy and spectrum $F(\mathbf{k})$ of elevations (ρ is the water density); ω is the intrinsic frequency of the wave; c is phase velocity of the wave; and Q_i are the sources describing different mechanisms of spectrum generation, such as influx from wind, wave breaking, viscous dissipation, nonlinear interaction waves, etc.

The required spectrum is the stationary solution of the kinetic equation when all the sources and sinks compensate for one another:

$$\sum_i Q_i(k,\theta) = 0. \qquad (2)$$

For calculations, we use an approach proposed in [12], where the spectrum is found by integrating nonstationary kinetic equation (1) with the help of an iterative method. The spectrum evolution is calculated before the stationary solution is found. However, our particular attention is drawn to a realistic description of the ways that the spectrum generates. To this end we introduce energy sources into Eq. (1) in line with [15] and calculate the three-wave interactions exactly as earlier using the techniques described in [9, 10].

In the model described in [15], the spectrum generation is determined by the following processes. The gravity waves are generated by wind and loss energy through the breaking of wave crests, which are accompanied with the formation of whitecaps and foam in the gravity range and with the generation of capillary waves propagating along the front slope of the breaking wave in the GC range. This process is called microwave breaking in the literature, and the resulting capillary waves are called a parasitic ripple [13, 14]. The short-wave energy is dissipated due to the action of viscosity. Another way for energy to transfer is by three-wave interactions. In the model described in [15], the three-wave interactions enter the kinetic equation (in view of dimensionality) as a sink proportional to the square of spectrum, which makes it possible to balance the strong energy influx in the capillary interval from the generation mechanism of parasitic capillaries. In our calculations, we change the parametrization for three-wave interactions by an exactly calculated integral of collisions. For all other sources, the same expressions as in [15] are used.

The dissipation due to molecular viscosity is taken into account in the traditional form $Q_\nu = 4\nu k^2 N(k, \theta)$ where ν is the kinematic water-viscosity coefficient. The influx from wind is taken to be in the form (see [15] and the references therein for details)

$$Q_{\text{wind}} = \omega\beta(\mathbf{k})N(\mathbf{k}), \qquad (3)$$

$$\beta(\mathbf{k}) = c_\beta(u_*/c)^2\cos\theta|\cos\theta|), \qquad (4)$$

where c is the phase velocity, u_* is the friction velocity in air, θ is the angle between the directions of wave vector and wind, c_β is the parameter of the wave growth rate (it is a function of k, but, in the given spectral range, is equal on average to 0.03). The source in Eq. (1) corresponding to nonlinear energy losses in the model [15] is expressed as

$$Q_{\text{diss}}(\mathbf{k}) = \omega^2 k^{-5} B(\mathbf{k}) \left(\frac{B(\mathbf{k})}{\alpha}\right)^n, \quad (5)$$

where $B(k, \theta) = k^4 F(k, \theta)$ is the Phillips saturation spectrum [19] or curvature spectrum. The parameters α and n are the main model parameters [14, 15], the values of which for different spectral intervals are determined by the dominant energy-loss mechanisms. The generation of the parasitic ripple is described using the following approach. The short gravity waves generating parasitic ripple during microwave breaking provide the energy transfer from the gravity to capillary range. The wave vectors of capillary $\mathbf{k}$ and generating gravity wave $\mathbf{k}_g$ are collinear and associated by the condition of phase synchronism $k_g = k_\gamma^2/k$, where $k_\gamma = \sqrt{g/\gamma}$ is the wave number of the phase-velocity minimum and γ is the coefficient of surface tension. The corresponding term of the kinetic equation has the form

$$I_{pc}(k, \theta) = Q_{\text{diss}}(k_g, \theta) \left(\frac{k_\gamma}{k}\right)^2 \phi\left(\frac{k}{k_\gamma}\right), \quad (6)$$

where $Q_{\text{diss}}(k_g, \theta)$ is the source describing energy losses in a long wave given by formula (5) and $\phi(k/k_\gamma)$ is a filtering function, the physical meaning of which is that the parasitic capillaries cannot be generated by decimeter and longer waves whose energy is lost during wave breaking with whitecap generation.

The technique of spectrum calculation described in detail in [12] consists of the following main points. The initial spectrum is given on a two-dimensional grid uniform with respect to the natural logarithm of the wave number $\ln(k/k_\gamma)$ and to the angle relative to the wind direction θ. Equation (1) is integrated with respect to time until the steady-state is found using a two-step explicit scheme. In the basic calculations performed in [12], the spectrum evolution was calculated for waves with lengths from a centimeter to several tenths of millimeter and the spectrum of longer waves ($k < k_\gamma/\sqrt{2}$) was fixed. In this case, the resulting solutions were independent of the level and form of the initial spectrum and were determined only by the form of sources and boundary conditions.

We strictly fixed the spectrum in the gravity range in view of the emerging instability in the GC range. In this study we calculate the spectrum of short gravity waves, adding sources into the kinetic equation in turn and observing the change in the course of spectral evolution and the resulting solution. Finally, the contribution of each individual mechanism to the generation of the spectra of short wind waves will be estimated.

3. QUASI-INERTIAL REGIME AND INSTABILITY IN THE GC RANGE

3.1. Modeling Results

Let us consider the simplest case, when spectral evolution is determined (along with the three-wave interactions) by a single linear source: the sum of wind input and viscous energy sink. Within the frameworks of this study, we call this a quasi-inertial regime in view of its physical similarity with the inertial regime [6] because, in our case, the most intensive energy influx goes to gravity waves and energy losses due to viscosity are the strongest for the shortest waves. A calculation for this case was performed in [12], but its results were not presented because no stable stationary solution is found (as was shown analytically). The course of spectral evolution and development of instability are illustrated in Fig. 1. Hereafter, the spectra will be represented using saturation spectra $B(\mathbf{k})$ and the sources will be shown in a dimensionless form as $Q_i T/N$, where $T(k)$ is the wave period. To show the source describing the three-wave interactions in the logarithmic scale, we show its absolute value and the ranges of positive values are marked by + symbols. Figures 1a and 1b present the sections of spectra and sources along the wind direction and in dependence of wave numbers normalized to the wave number of the phase-velocity minimum k_γ. Figure 1 shows the initial time of spectral evolution and spectral distribution of sources for the initial spectrum given close by the level to the model spectrum [15] for the same wind velocity of 5 m/s. Let us note that, for the initial spectrum with a power dependence on k, the three-wave interactions have a characteristic form with a jump and sign change at the point $k = \sqrt{2}\, k_\gamma$ [9].

Under the action of sources, the spectral form starts to change mainly in the neighborhood of the phase-velocity minimum $k \sim k_\gamma$ (Fig. 1a, curve *3*). Here, the characteristic point is $k = k_\gamma/\sqrt{2}$, in the left of which the wave involved in the three-wave interactions exchanges energy exceptionally with two shorter waves and in the right of which the wave interaction within the triad is performed with both a shorter and a longer wave [12]. Because the typical behavior of the wave-action spectrum (the square of which enters the integral of collisions) is that is falls with the increase in the wave number, the three-wave interactions in the course of evolution become intense in the range $k > k_\gamma/\sqrt{2}$ and almost inessential for wave $k < k_\gamma/\sqrt{2}$. Thus, at the point $k = k_\gamma/\sqrt{2}$, the spectrum is sharply separated into a longwave (increasing under the action of wind) part and a high-frequency (falling to zero) part,

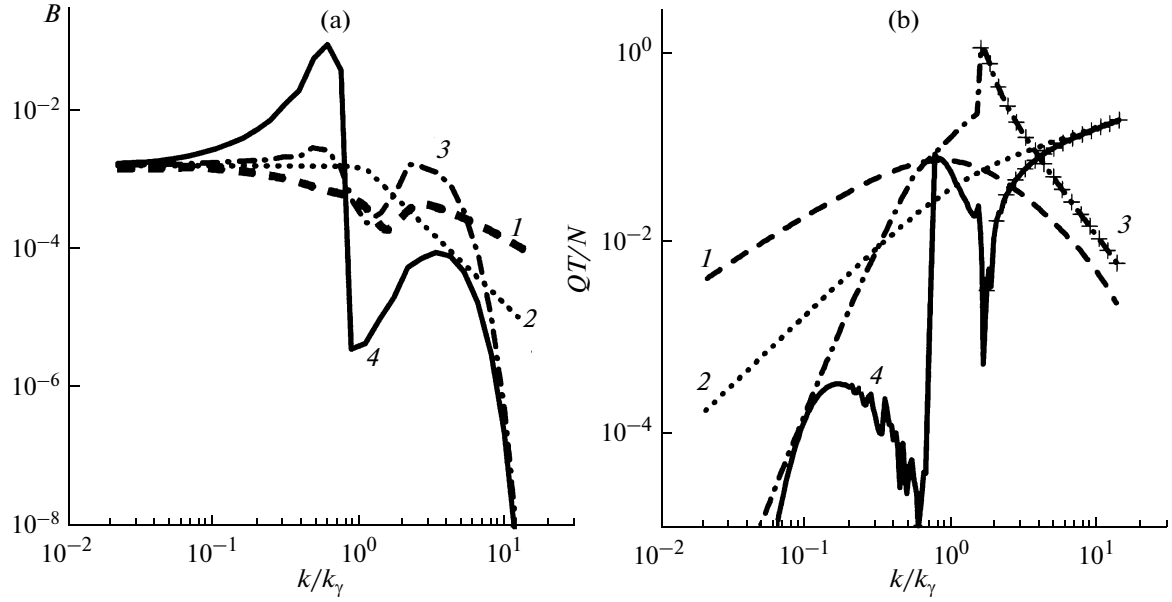

Fig. 1. Evolution of spectrum and sources in the quasi-inertial regime for a wind velocity of 5 m/s. (a) The calculated spectrum at 0 s (*2*), 1.2 s (*3*), and 6 s (*4*) in comparison with spectrum [15] (*1*). (b) Influx from wind (*1*), viscous dissipation (*2*), and three-wave interactions at 0 s (*3*) and 6 s (*4*). + symbols mark positive-source ranges.

where the three-wave interactions lead to a more powerful energy sink than its influx from wind. As a result, the spectrum takes a zigzag form and continues to increase without limit in the range of gravity waves and to fall in the capillary range (Fig. 1a, curve *4*).

The evolution of instability changes its character if the wind velocity is increased to 10 m/s (Fig. 2). Here, on the contrary, the spectrum strongly increases from the right of $k = k_\gamma/\sqrt{2}$ and sharply decreases in the gravity range. When the spectrum of capillary waves increases, the sum three-wave interactions acting for $k > \sqrt{2}\,k_\gamma$ start to play an essential role [9] and the pattern of spectrum evolution becomes important. However, as in the case of previous calculations, the instability continues to develop and no stationary solution is found (Fig. 2a, curve *4*).

If the wind velocity or the level and slope of the initial spectrum are changed, one of the above-mentioned types of instability also appears in line with analytic investigations in [12].

3.2. Need for Consideration of Nonlinear Dissipation

In [12], it has been revealed that, for the set of sources corresponding to the previous calculation, the instability disappears if one reduces the calculation range from the side of long waves starting with $k = k_\gamma/\sqrt{2}$. Therefore, the spectrum was separated into a diagnostic part ($k \le k_\gamma/\sqrt{2}$) where its level remains unchanged and a prognostic part ($k > k_\gamma/\sqrt{2}$) for which the spectral evolution was calculated. With reasoning similar to [12], we will show that this limitation can be eliminated by adding a nonlinear dissipation term in the GC range of the spectrum into the kinetic equation. Then, the stable solution can exist when the calculation is extended to a range of longer waves.

Let us estimate the expression for the three-wave interactions in ranges 0, 2, and 1 corresponding to the intervals $k_0 < k_\gamma/\sqrt{2}$, $k_\gamma/\sqrt{2} < k_2 < \sqrt{2}\,k_\gamma$, and $k_1 > \sqrt{2}\,k_\gamma$. In the intervals 0 and 2, only difference processes are possible [9]; here, the subintegral function is proportional to the expression

$$I_{\text{res}} \sim N_1 N_2 - N_0(N_2 - N_1), \tag{7}$$

where the following notations are used for brevity: $N_1 = N(k_1)$, $N_2 = N(k_2)$, and $N_3 = N(k_3)$, and the condition of resonance for difference processes are satisfied: $k_0 = k_1 - k_2$. Because $k_0 < k_2 < k_1$ and the wave-action spectra decrease rapidly with the growth of k, one can disregard all the terms in combination of spectra (7) except for $N_0 N_2$. Then, with account for the linear flux from wind (in the sum with viscous sink) $b_i N_i$ as well as nonlinear dissipation $c_i N_i^m$ the kinetic equation can be written approximately as

$$\begin{aligned} \frac{dN_0}{dt} &= b_0 N_0 - a_0 N_0 N_2 - c_0 N_0^{m_0}, \\ \frac{dN_2}{dt} &= b_2 N_2 - a_2 N_2 N_0 - c_2 N_2^{m_2}, \end{aligned} \tag{8}$$

where a and c are positive coefficients and $m > 1$.

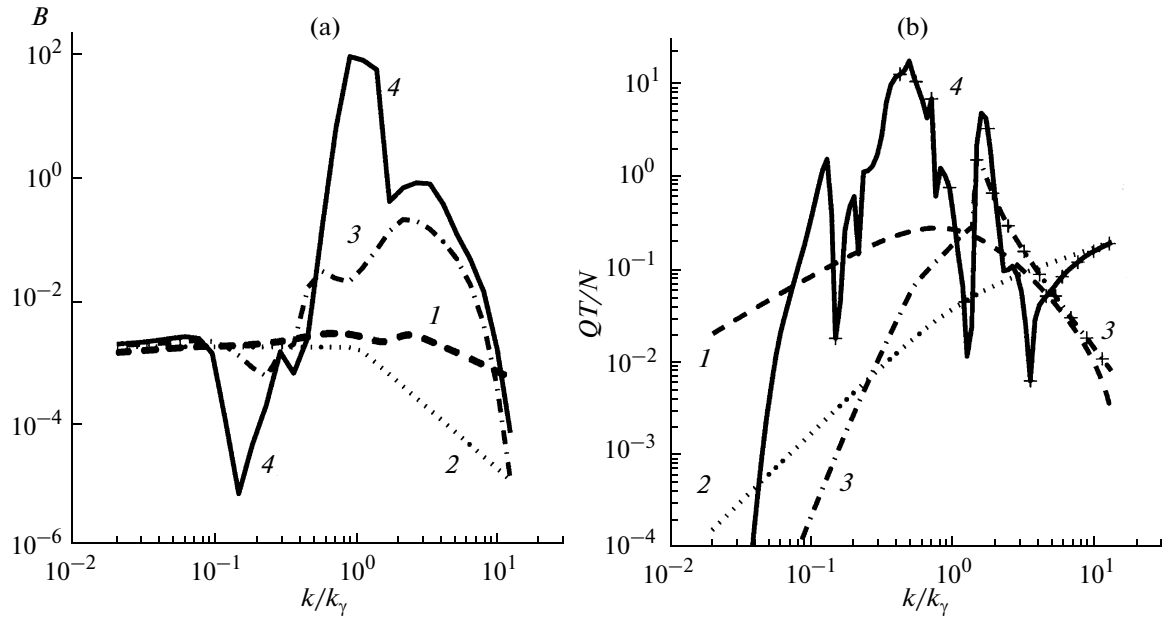

Fig. 2. Evolution of the spectrum and sources in the quasi-inertial regime for a wind velocity of 10 m/s. (a) The calculated spectrum at 0 s (*2*), 1 s (*3*), and 1.4 s (*4*) in comparison with spectrum [15] (*1*). (b) Influx from wind (*1*), viscous dissipation (*2*), and three-wave interactions at 0 s (*3*) and 1.4 s (*4*). + symbols mark positive-source ranges.

Let system (8) have a stationary solution $((\overline{N}_0,\ \overline{N}_2)$, i.e.,

$$b_0 - a_0\overline{N}_2 - c_0\overline{N}_0^{m_0-1} = 0,$$
$$b_2 - a_2\overline{N}_0 - c_2\overline{N}_2^{m_2-1} = 0.$$

Let us investigate the stability of this solution relative to minor disturbances ΔN_0 and ΔN_2. The equations for them accurate to linear terms are written in the form

$$\frac{d\Delta N_0}{dt} = -a_0\overline{N}_0\Delta N_2 - c_0(m_0-1)\overline{N}_0^{m_0-1}\Delta N_0,$$
$$\frac{d\Delta N_2}{dt} = -a_2\overline{N}_2\Delta N_0 - c_2(m_2-1)\overline{N}_2^{m_2-1}\Delta N_2, \quad (9)$$

where all the coefficients before ΔN_0 and ΔN_2 are negative. Let us denote

$$d_1 = c_0(m_0-1)\overline{N}_0^{m_0-1},\quad f_1 = a_0\overline{N}_0,\quad d_2 = a_2\overline{N}_2,$$
$$f_2 = c_2(m_2-1)N_2^{m_2-1}.$$

The disturbances ΔN_0 and ΔN_2 will exponentially attenuate with time if all roots of the characteristic equation of the system of linear differential equations (9) have negative real parts. The roots $s_{1,2}$ of the characteristic equation $(s + d_1)(s + f_2) = d_2f_1$ are negative for $d_1f_2 > d_2f_1$; i.e., the instability disappears if the inequality is satisfied:

$$c_0\overline{N}_0^{m_0}c_2\overline{N}_2^{m_2} > \frac{a_0\overline{N}_0^2}{m_0-1}\frac{a_2\overline{N}_2^2}{m_2-1},$$

or

$$c_0\overline{N}_0^{m_0}c_2\overline{N}_2^{m_2} > \frac{b_0\overline{N}_0}{2(m_0-1)}\frac{b_2\overline{N}_2}{2(m_2-1)}. \quad (10)$$

It follows from the last inequality that the stability of solution requires nonlinear (nonvanishing) dissipation and that there is a lower boundary for its absolute value. For example, for $m = 2$, the nonlinear dissipation must be (in its magnitude) no less than half of the flux from wind. For higher values of m, condition (10) becomes less strict.

4. MECHANISMS SHAPING THE SPECTRUM

4.1. Inertial–Dissipative Regime

Let us introduce into the kinetic equation nonlinear sink of energy (5) in the range of short gravity and GC waves and consider the spectral evolution in the whole range of short waves.

The behavior of function Q_{diss} at different segments of the spectrum is controlled by parameters α and n, which are functions of the dimensionless wave number k/k_γ and represented in Fig. 3. In the gravity range, where the energy dissipation is associated to the wave wave breaking ($k < k_{wb} \approx 2\pi/0.15$ rad/m), α and n are

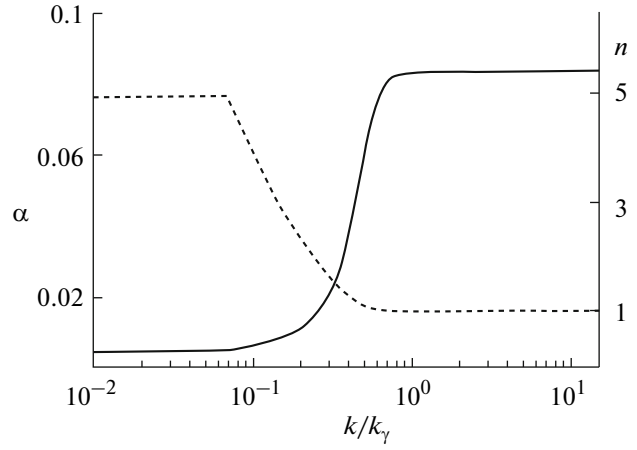

Fig. 3. Parameters α (solid line) and n (dashed line) in the expression for dissipation in model [15], depending on the wave number.

constants, particularly $n = 5$ as proposed in [20]. In the capillary range of spectrum ($k \gg 1/2k/k_\gamma$), these parameters must also be constants, but with other values. In the model [15], these values were proposed to be chosen so that the dissipation is quadratic by spectrum (i.e., $n = 1$), which corresponds to the expression for three-wave interactions written on the basis of dimensionality considerations. In the transition interval $k_{wb} < k < 1/2\,k/k_\gamma$, the energy losses are determined by microwave breaking and generations of parasitic capillaries. Here, both the gravity force and surface tension are equally important; therefore, α and n smoothly vary between their values in the capillary and gravity ranges.

At this stage of study, we turn on dissipation (5) only for the interval $k < \frac{1}{2}\frac{k}{k_\gamma}$ and turn it off in the remaining interval. Here, we assume that the three-wave interactions calculated in this interval should substitute the quadratic energy losses treated in [15] as their parametrization.

Let us consider the spectral evolution under the action of wind input, viscous dissipation, nonlinear dissipation in the range of short gravitation waves, and energy transfer by three-wave interactions in the whole range. In this case, due to the inclusion of additional nonlinear energy sink (in the longwave range $k < 1/2k/k_\gamma$) into the kinetic equation, the stationary solution really becomes steady-state.

The resulting spectra, along with spectra of model [15] for corresponding wind velocities, are shown in Fig. 4. For small wind velocities (5 m/s), the difference is essential only in the vicinity of the phase-velocity minimum, where a trough is generated in the saturation spectrum. This effect, which was also observed experimentally and related, apparently, to the action of three-wave interactions [21], was investigated in detail in [12]. However, with an increase in the wind velocity, another peculiarity appears: a characteristic zigzag; i.e., a sharp dip in the spectrum in the range of short gravity waves and a peak in the capillary range.

The approximate time it takes to establish this pattern is 5–10 s. During this time interval, the wind

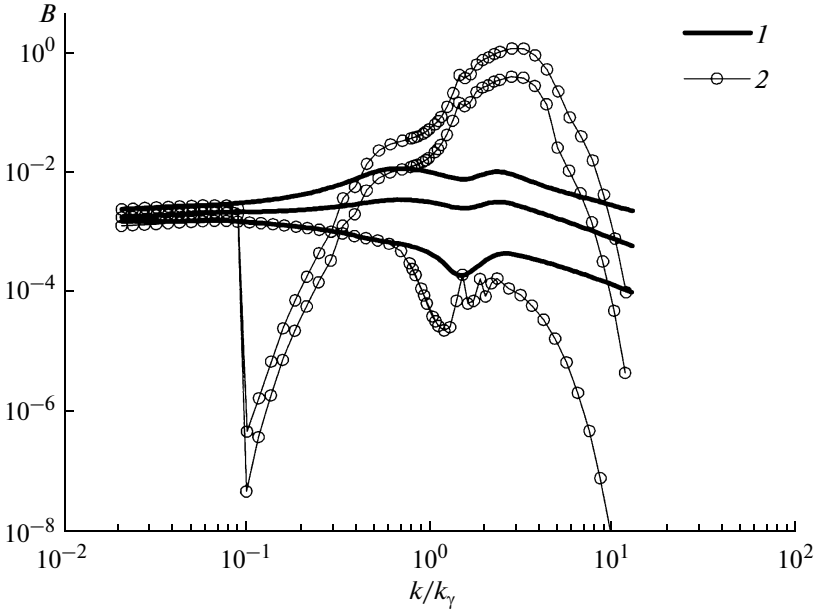

Fig. 4. The results of a calculation of (*2*) for the case of a balance for influx from wind, viscous dissipation, three-wave interactions, and dissipation related to the breaking of short gravity waves in comparison with spectra of model [15] (*1*). The wind velocities (from the bottom up) are 5, 10, and 20 m/s.

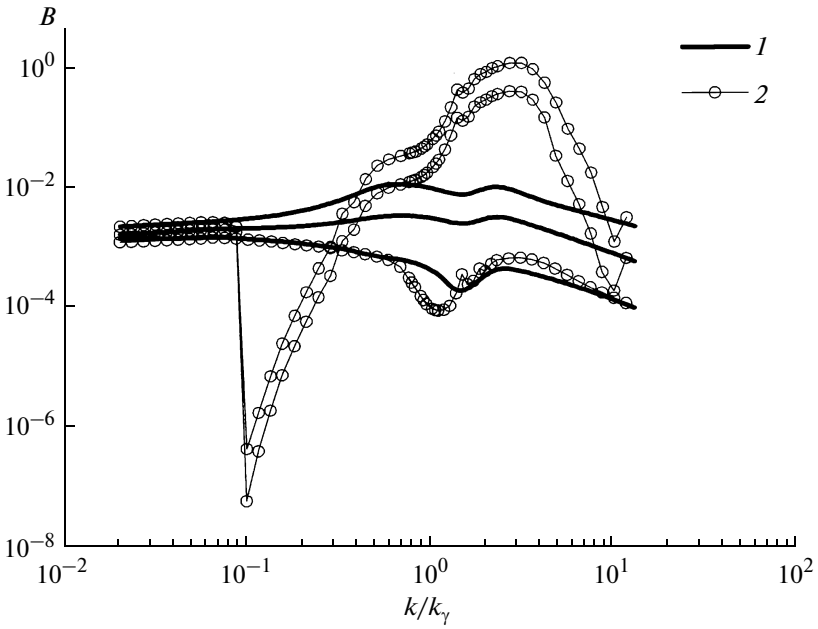

Fig. 5. The results of a calculation with account for the generation of parasitic ripple (*2*) in comparison with spectra of model [15] (*1*). The wind velocities (from the bottom up) are 5, 10, and 20 m/s.

influx of energy (which is sufficiently strong for both gravity and short waves) increases the level of spectrum in the GC range, where no nonlinear dissipation can be found and the energy sink is ensured merely by the action of liquid viscosity. The increased level of spectral energy intensifies the three-wave interactions in this range (since the integrand of the integral of collisions includes squares of the spectrum), and, as a result, the spectrum value here grows more strictly to unrealistically large values. The viscous dissipation alone turns out to be insufficient for compensating the three-wave energy influx so that the resulting spectrum has a reasonable order of magnitude. With an increase in the spectrum level of capillary waves, the three-wave interactions pump out the energy of the longwave range all the more strongly; as a result, the spectrum dips and generates a sharp minimum, which very slowly shifts towards a decrease in the wave number.

Thus, at large wind velocities, instability develops again. In addition, it can be seen from Fig. 4 that the spectral level of the shortest capillary waves ($k \sim 10k_\gamma$) is underestimated when compared to the results of model [15]; i.e., it is necessary to take into account the additional energy influx induced, for example, by the generation of parasitic capillary ripple.

Thus, the given spectral model requires new energy sources–sinks to be included.

4.2. Account of Parasitic Capillary Waves

Let us add into the kinetic equation a term describing the way that the parasitic capillary waves in form (6) generate. As a result, noticeable changes in the distribution of spectral energy occurred only in the range of the largest wave numbers, where the level of spectrum increases up to values consistent with the data obtained by model [15] (see Fig. 5). However, the pattern for the spectrum in the gravity and GC ranges remained the same as previously. The small jump of spectrum in the range $k/k_\gamma \sim 10$ at wind velocities of 10 and 20 m/s is evidently a response to the spectral form in the gravitation range: the stepwise increase in the level of spectral energy at $k/k_\gamma < 0.1$ sharply amplifies the generation of parasitic capillary waves with wave numbers $k/k_\gamma > 10$.

Thus, at this stage of study, the model incorporates all energy sources–sinks discussed in [15]. However, the spectrum of short waves remains unstable due to three-wave interactions. Let us note that, unlike the GC range, in the capillary range one cannot perform a simple stability analysis for the stationary solution of the kinetic equation because the estimation of three-wave interactions requires the use of an additional integral describing the sum processes [9], which highly complicates the analytical consideration. The conclusion that the energy sources–sinks in the given model cannot be balanced follows from numerical calculations.

4.3. Nonlinear Energy Dissipation in the Capillary Range

The calculations performed indicate that, in order to eliminate the observed instability, one needs an

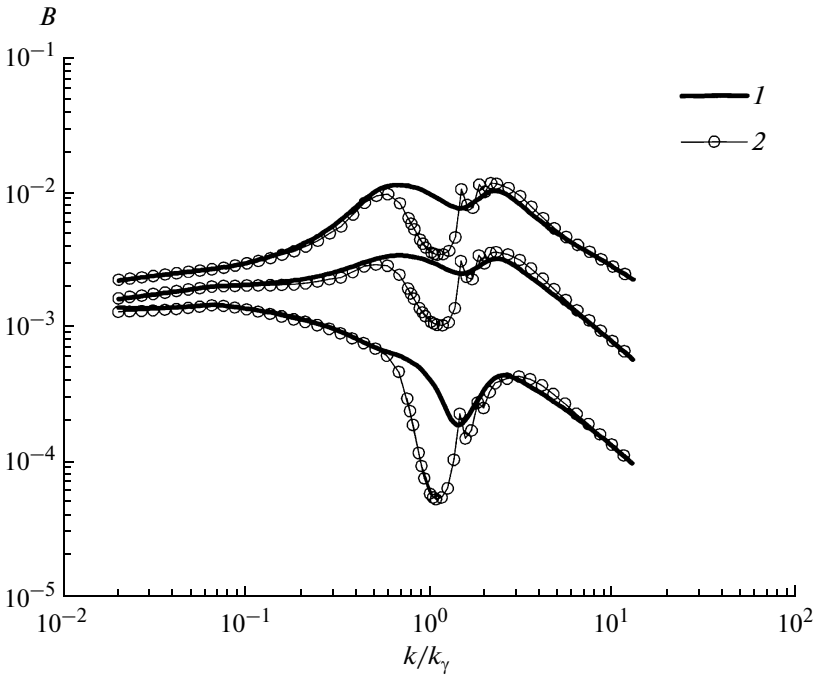

Fig. 6. The results of including nonlinear dissipation in the capillary range into the kinetic equation. The notations are the same as in Fig. 5.

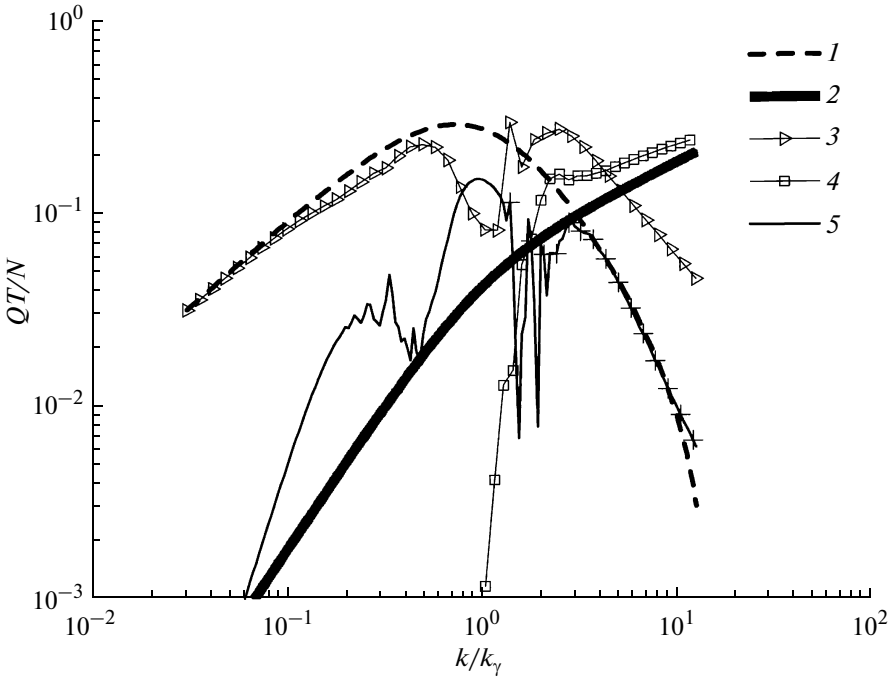

Fig. 7. Contributions of different physical mechanisms to the generation of stationary spectrum for a wind velocity of 10 m/s. (*1*) wind input, (*2*) viscous dissipation, (*3*) nonlinear dissipation, (*4*) generation of parasitic ripple, and (*5*) three-wave interactions. + simbols mark positive-source ranges.

additional dissipation mechanism limiting the spectral growth in the capillary range. Let us note that the model described in [15], in spite of its incorrect account of three-wave interactions, leads nevertheless to realistic spectra of short waves for different wind velocities. Consequently, leaving the integral of colli-

sions in the kinetic equation, in the shortwave range we return the nonlinear quadratic energy sink (treated in [15] as an analog of three-wave interactions), but now we treat this term as a nonlinear mechanism suppressing the strong growth of the spectral energy density of capillary waves. This mechanism can be represented, for example, by collapsed neighboring slopes of a capillary wave and a newly generated bubble of air over the trough when a critical wave curvature is reached. The existence of this phenomenon in capillary waves was theoretically predicted by Crapper [22]. However, the corresponding expression for dissipation was not considered earlier; therefore, it is natural to retain (as a first step) the phenomenological dissipation parametrization proposed in [15]. Let us note that this parametrization implies that α and n are constant for $k > k_\gamma$. This choice corresponds to the results of [23], where it was theoretically found that the profile of nonlinear stationary GC waves with $k > k_\gamma$ has a form characteristic to Crapper's pure capillary waves (namely, it allows neighboring slopes to collapse).

When nonlinear dissipation (5) is added, no spectral instability appears in the range $k > k_\gamma$. The calculated spectra are presented in Fig. 6. For all wind velocities, they are almost the same as the spectra calculated without the integral of collisions, except for the range of phase-velocity minimum, with a persisting characteristic trough as in previous calculations.

4.4. Ratio of Contributions of Different Sources in Kinetic Equation

The plots in Fig. 7 demonstrate the characteristic ratio of different sources and sinks in the kinetic equation by the time of spectrum establishment. The stationarity of the resulting spectrum in a practical calculation means that the algebraic sum of sources approaches zero. In this case, the value of the corresponding function is several orders of magnitude lower than the level of the function of any of sources: $Q_{\text{sum}}(k)\dfrac{N(k)}{T(k)} \sim 10^{-4}$. A comparison of absolute values of sources confirms the conclusion that the three-wave interactions play a key role only in the range of the phase-velocity minimum $k \sim k_\gamma$, where they are negative and, together with nonlinear dissipation, balance the influx from wind. In the capillary range, the formation of the spectral energy balance is dominated by dissipation (viscous and nonlinear) and the generation mechanism of parasitic capillaries, while the contribution of the remaining mechanisms is negligible. In the range of short gravity waves, the three-wave energy transfer is also considerably weaker than the two other main sources (wind input and break-related dissipation).

5. CONCLUSIONS

In this study, on the basis a numerical spectrum model constructed in [12], we analyze the role of different physical mechanisms in the establishment of stationary spectra of short wind waves. We found that, when only linear sources and three-wave interactions are used, the stationary solution of the kinetic equation is unstable or the spectrum level at some segments is inconsistent with the values observed experimentally. Thus, we demonstrated the need to include additional nonlinear terms in ranges of both short gravity and capillary waves into the kinetic equation. The mechanism that we used adds additional dissipation in the form proposed in [15]. The physical meaning of nonlinear energy losses is treated differently for different spectral ranges. In the gravity and GC ranges, they include wave breaking and microwave breaking, respectively. The nature of the nonlinear dissipation of capillary waves remains unclear; it is possibly related to the popping of wave slopes and the formation of an air bubble in capillary waves of peak curvature as predicted by Crapper [22] (an analog of the break of gravity waves).

The calculations performed demonstrate that the role of three-wave interactions is essential in the course of establishing a spectral energy balance. The three-wave interactions provide the interaction between capillary and gravity segments of the GC range of wind waves, which may lead to specific instabilities when the total energy is concentrated either in capillary or gravity segments. It is the account of three-wave interactions that made it possible in this study to choose sources–sinks providing a spectral energy balance without leading to instability. However, after the spectrum is established, the three-wave interactions continue to be an essential contribution to the spectral energy balance only near the minimum of surface-wave phase velocity, generating a trough on the curvature spectrum. At the same time, in other ranges, the balance is yielded mainly between the energy influx from wind (or through the generation of a parasitic capillary ripple) and dissipation due to nonlinear losses (or molecular viscosity).

ACKNOWLEDGMENTS

This work was supported by INTAS, project no. 05-1000008-8014; by the Sixth EU Framework Programme for Research and Technological Development (FP6), project no. SST-5-CT-2006-031001 (MONRUK); by the Federal Task Program "World Ocean," project no. 01.420.1.2.0001; and by the Ukrainian National Foundation for Basic Research, project no. F28.6/025.

REFERENCES

1. V. N. Kudryavtsev and V. K. Makin, "Coupled Dynamics of Short Waves and the Airflow over Long Surface Waves," J. Geophys. Res. **101** (C12), 3209–3221 (2002).
2. A. S. Monin and V. P. Krasitskii, *Phenomena on the Ocean Surface* (Gidrometeoizdat, Leningrad, 1985) [in Russian].
3. M. A. Donelan and R. Wannikhof, "Gas Transfer at Water Surfaces. Concepts and Issues," in *Geophysical Monograph 127* (American Geophysical Union, Washington, DC, 2002), pp. 1–10.
4. V. Kudryavtsev, V. Shrira, V. Dulov, et al., "On the Vertical Structure of Wind-Driven Sea Currents," J. Phys. Oceanogr. **38**, N2144 (2008).
5. G. J. Komen, L. Cavaleri, M. Donelan, et al., *Dynamics and Modeling of Ocean Waves* (University Press, Cambridge, 1994).
6. V. E. Zakharov and N. N. Filonenko, "Weak Turbulence of Capillary Waves," Prikl. Mekh. Tekh. Fiz., No. 5, 62–67 (1967).
7. K. Van Gastel, "Imaging of X-Band Radar of Sub-Surface Features: A Nonlinear Phenomenon," J. Geophys. Res. **92** (C11), 11857–11865 (1987).
8. M. Stiassnie, "On the Equilibrium Spectrum of Gravity-Capillary Waves," J. Phys. Oceanogr. **26** (6), 1093–1098 (1996).
9. V. A. Dulov, "Weakly Nonlinear Energy Transfer in Gravitational–Capillary Range of Surface Waves. Spectrum Shape Effect," MGZh, No. 1, 21–31 (2001).
10. V. A. Dulov, "Nonconservative Weakly Nonlinear Interaction between Gravity and Capillary Waves," Izv. Akad. Nauk, Fiz. Atmos. Okeana **38** (3), 398–401 (2002) [Izv., Atmos. Ocean. Phys. **38** (3), 354–357 (2002)].
11. V. G. Polnikov, "Nonlinear Three-Wave Interactions in the System of Gravity-Capillary Waves in Water," Izv. Akad. Nauk, Fiz. Atmos. Okeana **41** (2), 253–266 (2005) [Izv., Atmos. Ocean. Phys. **41** (2), 228–241 (2005)].
12. V. A. Dulov and M. V. Kosnik, "Effects of Three-Wave Interactions in the Gravity-Capillary Range of Wind Waves," Izv. Akad. Nauk, Fiz. Atmos. Okeana **45** (3) 408–419 (2009) [Izv., Atmos. Ocean. Phys. **45** (3) 380–392 (2009)].
13. M. S. Longuet-Higgins, "The Crest Instability of Steep Gravity Waves: Or how do Short Waves Break?," in *The Air–Sea Interface. Radio and Acoustic Sensing, Turbulence and Wave Dynamics*, Ed. by M. A. Donelan et al. (Toronto: Univ. Toronto Press, 1996). pp. 237–246.
14. V. N. Kudryavtsev, V. K. Makin, and B. Chapron, "Coupled Sea Surface-Atmosphere Model. Pt 2. Spectrum of Short Wind Waves," J. Geophys. Res. **104** (C4), 7625–7639 (1999).
15. V. Kudryavtsev, D. Hauser, G. Gaudal, et al., "A Semiempirical Model of the Normalized Radar Cross-Section of the Sea Surface: 1. The Background Model," J. Geophys. Res. **108** (C3), 1–23 (2002).
16. V. Kudryavtsev, D. Hauser, and G. Gaudal, "A Semiempirical Model of the Normalized Radar Cross-Section of the Sea Surface: 2. Radar Modulation Transfer Function," J. Geophys. Res. **108** (C3), 1–16 (2003).
17. V. Kudryavtsev, D. Akimov, J. Johannessen, et al., "On Radar Imaging of Current Features: 1. Model and Comparison with Observations," J. Geophys. Res. **110** (CO716) 1–27 (2005).
18. J. A. Johannessen, V. Kudryavtsev, D. Akimov, et al., "On Radar Imaging of Current Features: 2. Mesoscale Eddy and Current Front Detection," J. Geophys. Res. **110** (NI717) 1–14 (2005).
19. O. M. Phillips, "Spectral and Statistical Properties of the Equilibrium Range in Wind-Generated Gravity Waves," J. Fluid Mech. **156**, 505–531 (1985).
20. M. A. Donelan and W. J. Pierson, "Radar Scattering and Equilibrium Ranges in Wind-Generated Waves with Application to Scatterometry," J. Geophys. Res. **92** (C5), 4971–5029 (1987).
21. T. Elfouhaily, B. Chapron, K. Katsaros, et al., "A Unified Directional Spectrum for Long and Short Wind-Driven Waves," J. Geophys. Res. **102** (C7), 15781–15796 (1997).
22. G. D. Crapper, "An Exact Solution for Progressive Capillary Wave of Arbitrary Amplitude," J. Fluid Mech. **2** (6), 532–540 (1957).
23. S. J. Hogan, "Some Effects of Surface Tension on Steep Water Waves. Pt. 2," J. Fluid Mech. **96** (3), 417–445 (1980).